

## Self-Delivering Microstructured Iota Carrageenan Spray Inhibits Fibrosis at Multiple Length Scales

Robinson, Thomas E.; Brunet, Mathieu Y.; Chapple, Iain; Heagerty, Adrian H. M.; Metcalfe, Anthony D.; Grover, Liam M.

DOI:

[10.1002/anbr.202300048](https://doi.org/10.1002/anbr.202300048)

License:

Creative Commons: Attribution (CC BY)

### Document Version

Publisher's PDF, also known as Version of record

### Citation for published version (Harvard):

Robinson, TE, Brunet, MY, Chapple, I, Heagerty, AHM, Metcalfe, AD & Grover, LM 2023, 'Self-Delivering Microstructured Iota Carrageenan Spray Inhibits Fibrosis at Multiple Length Scales', *Advanced NanoBiomed Research*, vol. 3, no. 9, 2300048. <https://doi.org/10.1002/anbr.202300048>

[Link to publication on Research at Birmingham portal](#)

### General rights

Unless a licence is specified above, all rights (including copyright and moral rights) in this document are retained by the authors and/or the copyright holders. The express permission of the copyright holder must be obtained for any use of this material other than for purposes permitted by law.

- Users may freely distribute the URL that is used to identify this publication.
- Users may download and/or print one copy of the publication from the University of Birmingham research portal for the purpose of private study or non-commercial research.
- User may use extracts from the document in line with the concept of 'fair dealing' under the Copyright, Designs and Patents Act 1988 (?)
- Users may not further distribute the material nor use it for the purposes of commercial gain.

Where a licence is displayed above, please note the terms and conditions of the licence govern your use of this document.

When citing, please reference the published version.

### Take down policy

While the University of Birmingham exercises care and attention in making items available there are rare occasions when an item has been uploaded in error or has been deemed to be commercially or otherwise sensitive.

If you believe that this is the case for this document, please contact [UBIRA@lists.bham.ac.uk](mailto:UBIRA@lists.bham.ac.uk) providing details and we will remove access to the work immediately and investigate.

# Self-Delivering Microstructured Iota Carrageenan Spray Inhibits Fibrosis at Multiple Length Scales

Thomas E. Robinson,\* Mathieu Y. Brunet, Iain Chapple, Adrian H. M. Heagerty, Anthony D. Metcalfe, and Liam M. Grover

Fibrotic diseases account for 45% of all deaths in the developed world, and progressive scarring conditions, such as dystrophic epidermolysis bullosa (EB), result in a significant reduction in quality of life. There is thus a need for novel approaches in fibrosis prevention. Herein, it is shown that iota carrageenan, a low-cost, regulatory approved polysaccharide, is effective at preventing scarring by inhibiting collagen fibrillogenesis, abrogating the transforming growth factor beta 1 (TGF $\beta$ 1) pathway, and lubricating the epithelium. It is demonstrated that iota carrageenan, and other anionic polysaccharides, can prevent collagen fibril formation, a key step in scar formation. It also binds TGF $\beta$ 1 to prevent myofibroblast transdifferentiation, evidenced by a significant reduction in both transcription and translation of collagen 1 and alpha smooth muscle actin. Iota carrageenan may be formulated as a microparticle suspension, to allow spraying for even coverage on hard-to-reach anatomical sites, like the oral mucosa. This formulation provides good lubrication, to reduce the shear forces that initiate the progressive oral scarring in EB. This study not only provides a novel therapy for fibrosis prevention, but also demonstrates the potential of self-delivering immunomodulatory polysaccharides as a safe, cost-effective, and stable platform, which can be more easily translated for clinical benefit.

can lead to blindness,<sup>[8,9]</sup> and fibrosis in other organs, including the lungs,<sup>[10]</sup> liver,<sup>[11]</sup> and kidneys,<sup>[12]</sup> can be fatal; indeed, up to 45% of all deaths in the developed world are caused by fibrotic conditions.<sup>[13]</sup>

In addition to acute inciting events, such as burns, trauma, and surgery, dermal and mucosal scarring can also result from persistent chronic vesiculobullous conditions. Mucous membrane pemphigoid, an autoimmune condition affecting around two people per million per year, causes lesions that can lead to scarring in the eyes, nose, larynx, esophagus, genitals, and anus.<sup>[14,15]</sup> Interestingly, while this condition commonly presents with oral mucosal lesions, these do not typically scar; indeed, the oral mucosa is one of the few anatomical locations that does not scar in healthy humans.<sup>[1,7]</sup> Notable exceptions are sufferers of epidermolysis bullosa (EB), which is a heterogenous group of genetic conditions that lead to epithelial fragility and blister formation with only minimal trauma.<sup>[16]</sup>


## 1. Introduction

A key role of the epithelium is to act as a barrier to the external environment, and it is therefore vital that damage is repaired quickly and effectively.<sup>[1]</sup> To close the wound and restore this ectodermal barrier quickly, wound healing almost always results in a scar.<sup>[2,3]</sup> While many are innocuous, excessive scarring, for example following burn injury, can cause both physical impairment and psychosocial harm.<sup>[1,4–7]</sup> Scarring in the eye

In addition to marked effects on the skin and other areas, dystrophic EB can cause severe intraoral blistering, leading to excessive scar formation that can progress to ankyloglossia, microstomia, and obliteration of the oral vestibule.<sup>[16,17]</sup> This can further lead to difficulties maintaining sufficient nutrition and oral hygiene, increasing risk for dental caries and periodontal disease.

Because scarring is an innate component of wound healing, which is a multistage series of overlapping phases with an

T. E. Robinson, M. Y. Brunet, A. D. Metcalfe, L. M. Grover  
Healthcare Technologies Institute  
School of Chemical Engineering  
University of Birmingham  
Edgbaston, Birmingham B15 2TT, UK  
E-mail: T.E.Robinson@bham.ac.uk

 The ORCID identification number(s) for the author(s) of this article can be found under <https://doi.org/10.1002/anbr.202300048>.

© 2023 The Authors. Advanced NanoBiomed Research published by Wiley-VCH GmbH. This is an open access article under the terms of the Creative Commons Attribution License, which permits use, distribution and reproduction in any medium, provided the original work is properly cited.

DOI: 10.1002/anbr.202300048

I. Chapple  
School of Dentistry  
University of Birmingham  
Edgbaston, Birmingham B5 7EG, UK

I. Chapple  
Periodontal Service  
Birmingham Community Healthcare Foundation Trust  
Birmingham B7 4BN, UK

A. H. M. Heagerty  
Institute of Inflammation and Aging  
University of Birmingham  
Edgbaston, Birmingham B15 2TT, UK

ever-changing chemical, biological, and material environment, it can be difficult to pinpoint a specific factor as being responsible for pathological fibrosis. However, a key cytokine frequently implicated in aberrant scarring is transforming growth factor beta 1 (TGFβ1). This growth factor is widely considered profibrotic and is present in high levels in scar tissue.<sup>[18,19]</sup> TGFβ1 is released primarily from platelets and, once activated, binds to its receptors to trigger fibroblast-to-myofibroblast transdifferentiation, primarily through the suppressor of mothers against decapentaplegic (SMAD) 2/3,4 pathway (**Figure 1**).<sup>[20,21]</sup> Myofibroblasts, characterized chiefly by alpha smooth muscle actin (αSMA) expression, are responsible for collagen deposition and extracellular matrix (ECM) contraction.<sup>[22]</sup> However, while in normal wound healing these activated cells disappear following wound closure, in fibrosis they persist, with further ECM production and contraction leading to additional TGFβ1 release, which in turn propagates myofibroblast transdifferentiation. Further, TGFβ1 has a natural affinity for the ECM, leading to accumulation at sites of injury.<sup>[21]</sup> Thus, inhibiting TGFβ1 to terminate this positive feedback loop offers promise as a target to prevent fibrosis. However, systemic TGFβ1 inhibition causes serious issues with cardiac valves, systemic autoimmunity, and early death.<sup>[13,23]</sup> It is therefore vital that any TGFβ1 inhibitor be localized at the site of aberrant fibrosis. Many strategies have been employed to target TGFβ1 and prevent fibrosis, including TGFβ1 antibodies, peptides, and receptor decoys, however few result in positive patient outcomes.<sup>[24]</sup> Nonselective small molecules have shown the most effective and economical anti-fibrotic effects in vivo, though they are also more prone to side effects.<sup>[21]</sup>

Polysaccharides are widely used to prepare biomaterial delivery vehicles for therapeutic molecules.<sup>[25,26]</sup> While often

considered as inert carriers desirable only for their material and release properties, there is increasing evidence that many polysaccharides have inherent immunomodulatory functions.<sup>[27–31]</sup> Using polysaccharides can be advantageous because they are far more stable and more cost effective than biologics, and many have proven low toxicity, having been used in the food industry for decades.<sup>[32]</sup> Further, the microstructure of many polysaccharides can be manipulated to form hydrogels, microgels, and fluid gels.<sup>[33–35]</sup> Creating the delivery vehicle from the therapeutic itself allows these materials to be self-delivering, and containing only a single, regulatory approved component greatly eases clinical translation.

In this study, a range of common polysaccharides (shown in **Figure 2**) are investigated for their ability to prevent fibrosis at multiple length scales, including inhibiting collagen fibrillogenesis and TGFβ1-induced myofibroblast transdifferentiation. The most promising polysaccharide was then investigated to create a novel self-delivering, microstructured formulation, which can be sprayed to provide even coverage over hard-to-reach locations such as the oral mucosa, and provide lubrication to minimize the shear trauma that ultimately gives rise to oral scarring in EB.

## 2. Main

### 2.1. Inhibition of Collagen Fibrillogenesis

Fibrosis is the excessive laydown of ECM, primarily collagen type 1. The ability to delay or entirely prevent collagen fibril formation has been explored as a strategy to inhibit scar formation at the ECM level. The effect of several natural polysaccharides on collagen fibrillogenesis was thus tested in vitro. In the absence of any inhibitors, collagen formed fibrils at increased temperatures, forming a turbid gel over time (**Figure 3A**). However, some natural polysaccharides were able to slow down, or entirely prevent, this process. Specifically, at concentrations above 0.00125%, gellan (**Figure 3B**), iota carrageenan (**Figure 3C**), dextran sulfate (DS) (**Figure 3D**), and alginate (Alg) (**Figure 3E**), which are all anionic, appeared to completely inhibit fibrillogenesis. Interestingly, methyl cellulose (MC), an uncharged polymer, had no significant effect on collagen fibrillogenesis at any tested concentration (**Figure 3F**,  $p > 0.05$ ). This suggests that the negative charge carried by many of these polysaccharides is crucial to inhibiting collagen fibrillogenesis.

The effect of the polymer concentrations that did not entirely prevent fibrillogenesis were analyzed by comparing the time taken to reach 95% of the plateau to that of the water only control (38 min) (**Figure 3G**). Despite being able to inhibit gelation at high concentration, gellan did not significantly slow fibrillogenesis below 0.000125%. At 0.000125%, iota carrageenan (123 min,  $p < 0.0001$ ) and DS (119 min,  $p < 0.0001$  at 0.000125%, 59 min,  $p < 0.01$  at 0.0000125%) significantly retarded collagen fibrillogenesis, as did Alg (79 min,  $p < 0.0001$  at 0.000125%, 68 min,  $p < 0.0001$  at 0.0000125%). This shows that, at low concentrations, iota carrageenan and DS are the most effective, suggesting that in addition to negative charge, the possession of sulfate groups specifically may be important to prevent fibrillogenesis. Interestingly, proteoglycans and glycosaminoglycans, molecules

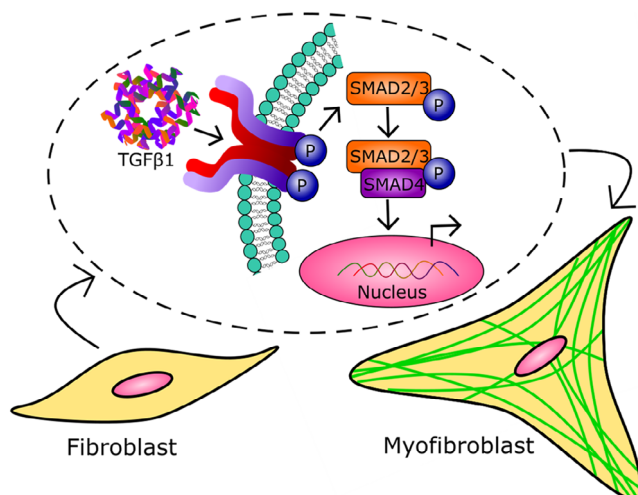


**Figure 1.** Transforming growth factor beta 1 (TGFβ1) induces myofibroblast transdifferentiation. A simplified schematic of the TGFβ1 signaling pathway. Following release and activation, TGFβ1 binds to its receptors on the fibroblast cell, triggering a phosphorylation (P) cascade culminating in the phosphorylation of suppressor of mothers against decapentaplegic (SMAD)2 or SMAD3. This phosphorylation leads to complexation with SMAD4 and translocation to the nucleus, binding to gene promoters and activating transcription of, among others, collagen 1 (COL1) and alpha smooth muscle actin (αSMA). Not shown are pathway inhibitors, such as SMAD7, or alternative pathways.

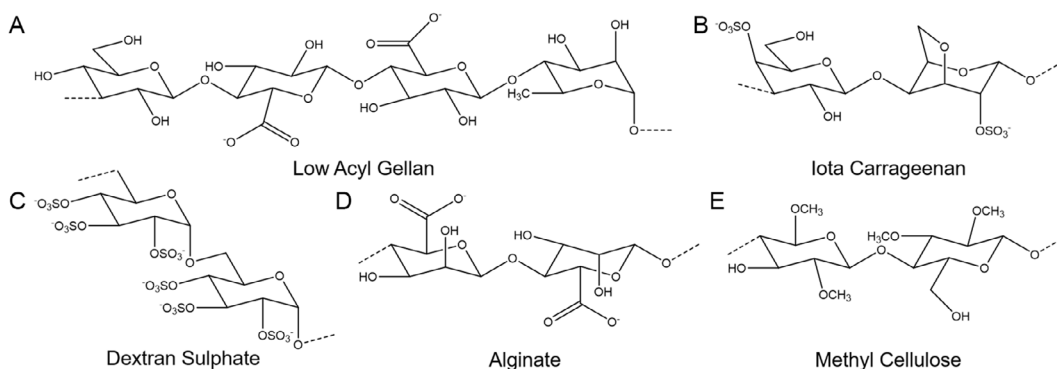


**Figure 2.** Structures of natural polysaccharides. The chemical structure of A) low acyl gellan, B) iota carrageenan, C) dextran sulfate, D) alginate, and E) methyl cellulose.

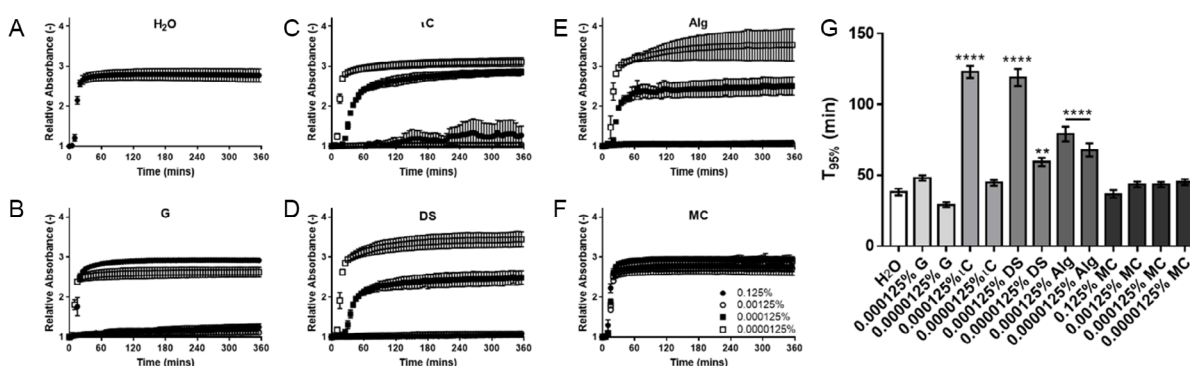


**Figure 3.** Anionic polymers inhibit collagen fibrillogenesis. The change in 405 nm absorbance over time of mixtures of collagen, phosphate buffered saline (PBS) and A) water, B) gellan (G), C) iota carrageenan (iC), D) dextran sulphate (DS), E) alginate (Alg), and F) methylcellulose (MC). An increase in relative absorbance indicates collagen fibril formation. G) The time taken to reach 95% of the plateau value for polysaccharide concentrations that did not completely inhibit fibrillogenesis. All figures show the mean  $\pm$  SD ( $n = 3$ ).

implicated in directing collagen fibrillogenesis in vivo, are often heavily sulfated.<sup>[36–38]</sup>

## 2.2. Prevention of Myfibroblast Transdifferentiation

Myfibroblasts, the cells responsible for rapid ECM production and contraction in fibrosis, are transdifferentiated from fibroblasts primarily through TGF $\beta$ 1 signaling (Figure 1). The ability to prevent fibroblasts from transdifferentiating into myfibroblasts should thus limit the overaccumulation of collagen associated with scarring. The ability of the polysaccharides to prevent fibrosis was tested in an in vitro model of scarring, where exposure to TGF $\beta$ 1-induced myfibroblast transdifferentiation.

A key feature of myfibroblasts is their increased collagen production compared to fibroblasts. At the genetic level, exposure to TGF $\beta$ 1 increased transcription of collagen 1 (COL1) twofold (Figure 4A, negative control (NC) versus positive control (PC),  $p < 0.01$ ). It was found that iota carrageenan ( $p < 0.0001$ ), Alg ( $p < 0.01$ ), and MC ( $p < 0.01$ ) significantly downregulated COL1 compared to the PC, with iota carrageenan having the greatest effect. Myfibroblasts are characterized primarily by increasing  $\alpha$ SMA expression; this form of actin gives them their contractile ability, and indeed it was demonstrated that TGF $\beta$ 1

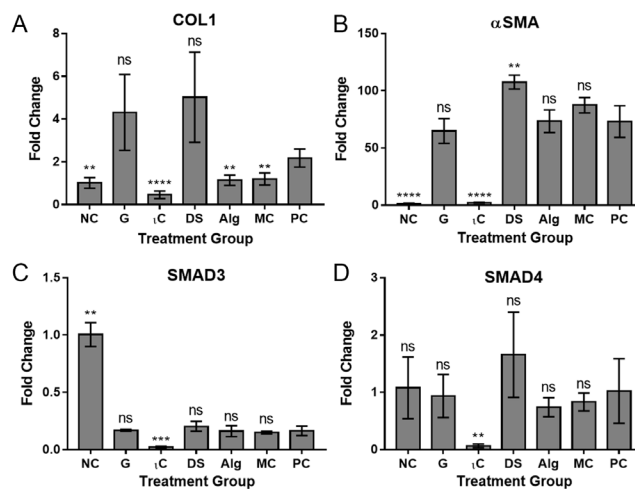


**Figure 4.** Iota carrageenan downregulates scarring genes. Fold-change in A) COL1, B)  $\alpha$ SMA, C) SMAD3, and D) SMAD4 mRNA levels, as measured by reverse transcription quantitative polymerase chain reaction (RT-qPCR), in fibroblasts exposed for 48 h to normal culture conditions (NC), media doped with 10 ng mL<sup>-1</sup> TGF $\beta$ 1 (PC), and media with TGF $\beta$ 1 plus gellan (G), iota carrageenan (iC), DS, Alg, and MC. All figures show mean  $\pm$  SD, statistical differences calculated using a  $t$ -test with Welch's correction, between each group ( $n = 3$ ) and PC ( $n = 6$ ).

induced a 73-fold increase in  $\alpha$ SMA gene transcription (Figure 4B, NC vs PC,  $p < 0.0001$ ). This was significantly reduced to only a twofold increase by iota carrageenan ( $p < 0.0001$ ), but was not significantly affected by the other polymers.

Binding of TGF $\beta$ 1 to its type II serine/threonine receptor, TGF $\beta$ R2, activates the type I receptor TGF $\beta$ R1, also termed activin receptor-like kinase 5, to intracellularly phosphorylate receptor-regulated SMAD proteins (R-SMADs).<sup>[39]</sup> Activated R-SMADs, such as SMAD3, form complexes with cofactor SMAD4 and these complexes translocate to the nucleus where they regulate gene transcription (Figure 1). This process is key to the TGF $\beta$ 1-induced signaling pathway of myfibroblast transdifferentiation. Interestingly, exposure to TGF $\beta$ 1 actually downregulated SMAD3 gene transcription (Figure 4C, NC vs. PC,  $p < 0.01$ ), a finding that has been noted previously.<sup>[40]</sup> Iota carrageenan, alone of the polymers tested, significantly dampened SMAD3 gene transcription further ( $p < 0.001$ ). In addition to the effect on the TGF $\beta$ 1 signaling pathway, this may be beneficial in itself, as it has been shown that mice lacking SMAD3 show accelerated wound healing.<sup>[41]</sup> SMAD4 gene transcription was also downregulated by iota carrageenan (Figure 4D,  $I < 0.01$ ), despite TGF $\beta$ 1 itself not having a significant effect.

In addition to downregulating transcription of key genes, it is important to show that this translates to the protein level, particularly for collagen 1 and  $\alpha$ SMA. Exposure to TGF $\beta$ 1 for 48 h induced extensive myfibroblast transdifferentiation, which could be visualized through immunocytochemistry by high  $\alpha$ SMA expression (Figure 5A). Quantification of immunocytochemistry images showed a significant increase in  $\alpha$ SMA protein

expression on exposure to TGF $\beta$ 1 (Figure 5B, NC vs PC,  $p < 0.0001$ ); however, this was significantly reduced by iota carrageenan ( $p < 0.0001$ ) and Alg ( $p < 0.01$ ). The change in collagen 1 protein expression could not be detected through immunocytochemistry quantification after 48 h (NC vs PC,  $p > 0.05$ , data not shown); however, a difference could be seen through quantitative picrosirius red staining (Figure 5C). This technique showed collagen production was increased by TGF $\beta$ 1 signaling (NC vs. PC,  $p < 0.01$ ), but was significantly reduced by iota carrageenan ( $p < 0.01$ ). While not statistically significant, Alg also appeared to slightly dampen collagen production.

The ability of the polysaccharides not only to prevent, but also to reverse the scarring response, was examined by exposing the fibroblasts to TGF $\beta$ 1 for 48 h (other than NC1), then changing to media without TGF $\beta$ 1 (other than PC) with the polysaccharides. Again, exposure to TGF $\beta$ 1 significantly increased  $\alpha$ SMA expression (Figure 5D, NC1 vs PC,  $p < 0.0001$ ). Interestingly, exposure to TGF $\beta$ 1 for 48 h then to normal, TGF $\beta$ 1-free media for 72 h produced the same response as exposure to TGF $\beta$ 1 for the full 5 days (NC2 vs PC,  $p > 0.05$ ). This suggests that initiation of myfibroblast transdifferentiation occurs quickly, and extended TGF $\beta$ 1 exposure has no effect, or that the myfibroblasts transdifferentiated by 48 h then produce TGF $\beta$ 1 themselves to propagate the process. The latter is supported by the greater absolute values of fluorescence intensity in the 5-day experiment compared to the 2 days for all groups exposed to TGF $\beta$ 1 (Figure 5B vs 5D). Further, autocrine production of TGF $\beta$ 1 has been observed previously in myfibroblasts, including those from hypertrophic scars.<sup>[42,43]</sup> Again, iota carrageenan ( $p < 0.01$ )

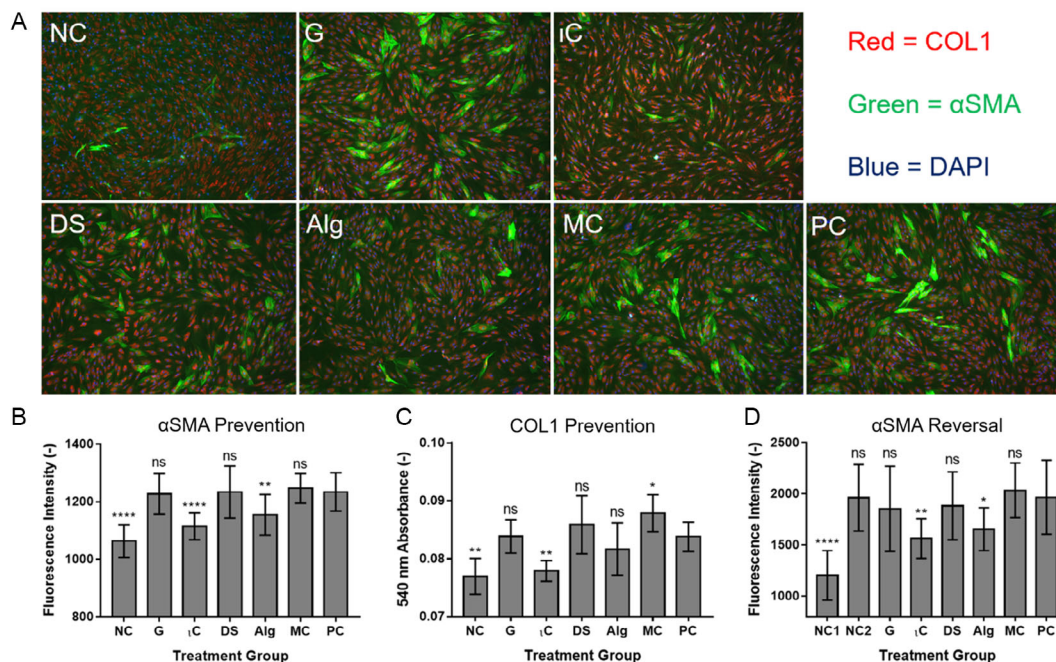


**Figure 5.** Iota carrageenan downregulates scarring proteins. A) Representative immunocytochemistry images of fibroblasts cultured for 48 h in normal culture conditions (NC), media doped with 10 ng mL<sup>-1</sup> TGF $\beta$ 1 (positive control [PC]), and media with TGF $\beta$ 1 plus gellan (G), iota carrageenan (iC), DS, Alg, and MC. B) Quantification of  $\alpha$ SMA from immunocytochemistry images. C) Quantification of collagen laydown after 48 h of culture by picrosirius red staining. D) Quantification of  $\alpha$ SMA from immunocytochemistry images taken after 5 days of NC1, 5 days in media doped with 10 ng mL<sup>-1</sup> TGF $\beta$ 1 (PC), 2 days in TGF $\beta$ 1 then 3 days in normal media (NC2), or media doped with gellan (G), iota carrageenan (iC), DS, Alg, and MC. In (B) and (D), mean  $\pm$  SD of >12 images, in (C), mean  $\pm$  SD ( $n = 6$ ), all statistical differences calculated using a  $t$ -test with Welch's correction between each group and PC.

and Alg ( $p < 0.05$ ) were able to reduce this response, though did not drive expression down as near to the previous NC baseline as in the prevention case (Figure 5B).

In the previous experiments (Figure 5), experimental media (containing polysaccharides and TGF $\beta$ 1) was created 24 h in advance of application to cells. To examine how the polysaccharides might be interacting with the system, the experimental media was made immediately prior to application and, interestingly, none of the polymers appeared to have a significant therapeutic effect (Figure 6A). This led to the hypothesis that the therapeutic effect was caused by interaction between the polysaccharides and TGF $\beta$ 1, rather than between the polysaccharides and receptors on the cell. Complexation between iota carrageenan and TGF $\beta$ 1 was studied directly by measuring the colloidal size of the polysaccharide and protein separately, and combined as in the cell system (Figure 6B). Iota carrageenan alone displayed two peaks, perhaps indicating the presence of unaggregated (at around 9 nm) and aggregated (at around 106 nm) polymers. TGF $\beta$ 1, meanwhile, displayed a single peak at 164 nm. The mixed system displayed both peaks for the iota carrageenan, as well as a third peak at 5560 nm. This suggests the formation of large aggregates from the combination of iota carrageenan and TGF $\beta$ 1.

Iota carrageenan forming a complex with TGF $\beta$ 1 would explain how it inhibits myofibroblast transdifferentiation at the molecular level (Figure 6C). This may be by covering the

active site on the protein that couples with the receptor on the cell, or sterically preventing binding between the protein and its receptor due to the size of the complex. While iota carrageenan was the most effective of the polysaccharides investigated, this mechanism is nonspecific, and may be extended to other polysaccharides, such as Alg, that also showed some efficacy. As the mechanism of binding is most likely electrostatic, between the positively charged protein and negatively charged polysaccharide, this suggests why MC, an uncharged polymer, had little effect in this study. This mechanism may also explain why iota carrageenan and Alg appear able to impede transdifferentiation once started (Figure 5D), as it can sequester the TGF $\beta$ 1 produced by the already transdifferentiated myofibroblasts, breaking the positive feedback loop and preventing further transdifferentiation.

### 2.3. Iota Carrageenan Formulation

Iota carrageenan appears to be highly effective at preventing fibrosis, both by inhibiting collagen fibril formation, and preventing myofibroblast transdifferentiation. Dilute solutions (0.005%) have material properties similar to water, yielding very low retention on the oral mucosa, while concentrated solutions (0.5%) spray poorly.<sup>[44]</sup> This has been overcome previously by blending with another polysaccharide to disrupt the bulk network.<sup>[44]</sup> Carrageenans undergo gelation by transitioning from random

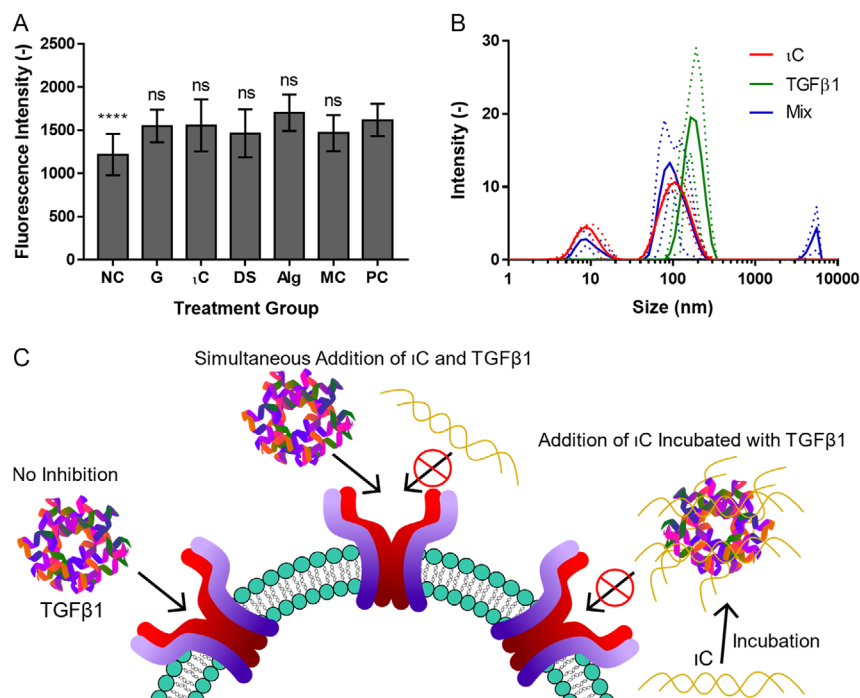


**Figure 6.** Iota carrageenan sequesters TGF $\beta$ 1. A) Quantification of  $\alpha$ SMA from immunocytochemistry images, where the polysaccharides were mixed with the TGF $\beta$ 1-containing media immediately prior to application for 48 h. Statistical differences calculated with respect to PC for each condition. B) Particle size distribution of iota carrageenan (red), TGF $\beta$ 1 (green), and their mixture (blue), measured in cell culture media by dynamic light scattering (DLS). C) Schematic of the suggested mechanism by which anionic polymers inhibit TGF $\beta$ 1 signaling: when applied simultaneously, TGF $\beta$ 1 binds strongly to its receptor before it can be sequestered by iC, and iC does not appear to interact with the receptor, however when premixed, iC complexes with TGF $\beta$ 1, preventing it from binding to its receptor. In (A), the mean  $\pm$  SD of >12 images, statistical differences calculated using a *t*-test with Welch's correction between each group and PC; in (B), mean (solid lines)  $\pm$  SD (dotted lines) ( $n = 3$ ).

coil structures when hot to double helices when cooled, which then aggregate to form a bulk network.<sup>[45]</sup> As polyanions, this process is influenced by the presence of cations. It was thus investigated whether cations, introduced under shear, could be used to create a particulate microstructure to facilitate improved spraying.

Without the addition of cations, 0.5% iota carrageenan solution was elastically dominated at all frequencies tested ( $G' > G''$ , **Figure 7A**). This showed that the polymers formed a bulk network capable of storing energy, and indicates bulk double-helix aggregation. Interestingly, the addition of high concentrations (0.5 M) of either NaCl (**Figure 7B**) or CaCl<sub>2</sub> (**Figure 7C**) to the solution prior to cooling under shear (NaCl-H and CaCl<sub>2</sub>-H, respectively) did not appear to alter this network structure, as the oscillatory rheological profiles appear similar. This also seems to be the case for NaCl added under shear to the iota carrageenan solution when cool (NaCl-C, **Figure 7D**). Only CaCl<sub>2</sub>, added to the cold solution under shear (CaCl<sub>2</sub>-C), appreciably altered the rheological profile, lowering both the elastic and viscous moduli (**Figure 7E**). This decreased stiffness suggests interruption of the bulk network structure, and indeed the phase angle is appreciably higher (data not shown) for CaCl<sub>2</sub>-C, suggesting that less energy can be stored in the system.

A similar trend was seen in the viscosity profile. Iota carrageenan solution was found to be shear thinning, with a high viscosity (100 Pa s) at low shear stress, which dropped almost four orders of magnitude at high shear stress (**Figure 7F**). The addition of sodium, either when hot (NaCl-H) or cold (NaCl-C), did not appreciably change this profile, and the addition of calcium when hot (CaCl<sub>2</sub>-H) appeared only to slightly reduce the stress required for shear thinning, but did not change the upper or lower viscosity thresholds. However, when added cold (CaCl<sub>2</sub>-C), calcium slightly reduced the low stress viscosity, but notably reduced the onset of shear thinning to a much lower stress value. This is likely because, rather than breaking the double-helix aggregates apart, which requires large forces, the shear

thinning in this system represents the disentanglement of individual particles, which requires notably less stress.

The microstructure of each formulation was assessed through light microscopy. In the absence of added cations (**Figure 8A**), NaCl-H (**Figure 8B**), CaCl<sub>2</sub>-H (**Figure 8C**), or NaCl-C (**Figure 8D**), no appreciable microstructure was visible. However, for CaCl<sub>2</sub>-C, a distinct microstructure was visible that appeared as small aggregates on the order of 1–10 μm in size (**Figure 8E**). At the macroscale, this microstructure was observable by a significant increase in turbidity (**Figure 8F**,  $p < 0.001$ ). This is indicative of the formation of large aggregates (observed in **Figure 8E**), a phenomenon previously observed in gellan, which also gels by formation and aggregation of double helices, at high calcium concentrations.<sup>[46]</sup> In iota carrageenan, increasing the calcium concentration above a critical value has been shown to increase the local heterogeneity and lead to phase separation.<sup>[47]</sup> Further, at comparable concentrations of both calcium and polymer used in this study, iota carrageenan has been shown to precipitate.<sup>[45]</sup> Here, by constantly mixing during this process, the precipitate has been blended in to yield the observed particulate microstructure. The high ionic forces that cause precipitation may prevent the polymers from rearranging, as they would in a “weak” gel conformation, from the formed microstructure. However, because the polymers in the precipitated areas are less swollen, and thus have a smaller hydrodynamic volume, polymer–solvent and polymer–polymer interactions are reduced, leading to slightly lower viscosity and moduli.

It is interesting that CaCl<sub>2</sub> causes this drastic change in microstructure, and thus material properties, only when added once the iota carrageenan is cold. It is well known that iota carrageenan has a higher affinity for divalent cations, such as calcium, than monovalent ones, such as sodium, and that divalent cations result in stronger, if still technically “weak,” gels.<sup>[45,47]</sup> It has been suggested that monovalent cations elicit intramolecular interactions only, increasing attraction within double helices rather than between them.<sup>[48–50]</sup> This may explain why NaCl formulations

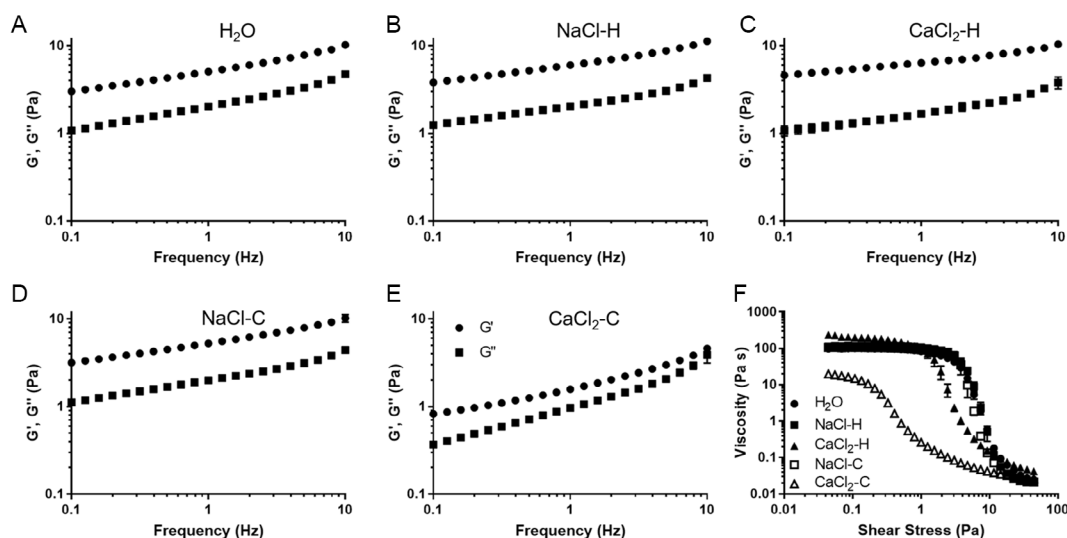


**Figure 7.** Rheological characterization of iota carrageenan formulations. Frequency sweeps of A) 0.5% iota carrageenan solution, 0.5% iota carrageenan solution mixed while hot with B) sodium (NaCl-H) and C) calcium (CaCl<sub>2</sub>-H), then cooled down under shear, and 0.5% iota carrageenan solution mixed following cooling with D) sodium (NaCl-C) and E) calcium (CaCl<sub>2</sub>-C). F) Shear stress ramps of these formulations. All figures show mean  $\pm$  SD ( $n = 3$ ).

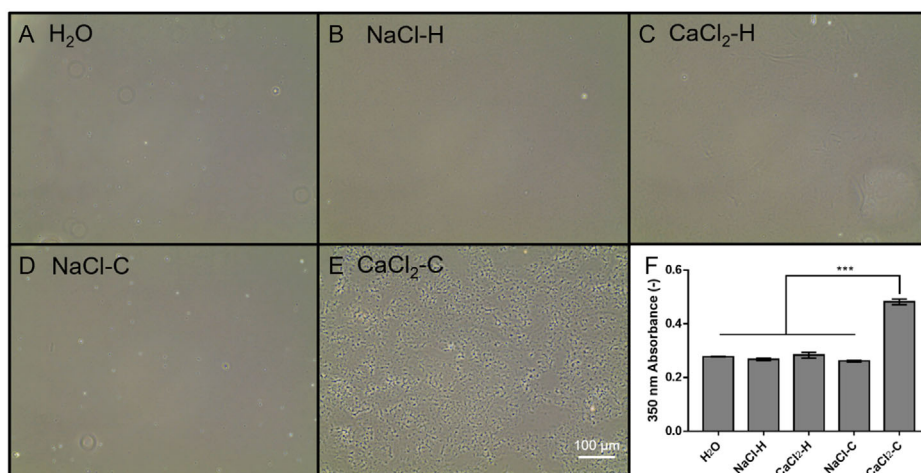


**Figure 8.** Structuring iota carrageenan with cations. Microscopy images of A) 0.5% iota carrageenan solution, 0.5% iota carrageenan solution mixed while hot with B) sodium (NaCl-H) and C) calcium (CaCl<sub>2</sub>-H), then cooled under shear, and 0.5% iota carrageenan solution mixed following cooling with D) sodium (NaCl) and E) calcium (CaCl<sub>2</sub>-C). F) Turbidity of each formulation, measured through its light absorbance; in F) mean  $\pm$  SD ( $n = 3$ ), statistical differences calculated using a *t*-test with Welch's correction between each group and CaCl<sub>2</sub>-C.

did not produce a notable microstructure, as the interhelical aggregation was not affected. Conversely, divalent cations are able to bridge neighboring double-helix structures, promoting such interhelical aggregation.<sup>[51]</sup> However, it has been suggested that intramolecular bridges may form preferentially to intermolecular ones.<sup>[49]</sup> It is thus hypothesized that, when added while the polymers are in a random coil formation in hot solution, calcium is bound to form intramolecular bridges during double-helix formation on cooling, and is therefore less available for interhelix aggregation. Conversely, when added after double-helix formation, the added calcium is available to form interhelical bridges, and aggregate the microstructure to such an extent that phase separation is induced. This would explain the marked differences between the formulations containing the same components, in the same concentrations, where only the formulation method differs.

#### 2.4. Formulation Sprayability and Lubrication

Spray delivery is a convenient way to provide an even layer of material to difficult-to-reach anatomical locations, such as the nasal and oral mucosa. By forming a microstructure and discretizing the polymers into small particles, such formulations may spray more readily than a bulk network. In dilute systems, where the polymers do not overlap and thus act as discrete particles, spray area was high (Figure 9A). Interestingly, even in this system, the addition of cations appeared to slightly increase spray area, though not significantly. This may be due to charge screening allowing increased intramolecular interaction, effectively decreasing particle size. In the concentrated system, iota carrageenan solution sprayed poorly, as previously noted, because the bulk polymer network cannot be disrupted sufficiently during the short spraying time.<sup>[44]</sup> Interestingly, even the formulations that did not alter the oscillatory or shear rheology, nor induce a visible microstructure, significantly increased the spray area (Figure 9B); approximately a fourfold increase for NaCl-H ( $p < 0.01$ ), a twofold increase for CaCl<sub>2</sub>-H ( $p < 0.05$ ), and a

fivefold increase for NaCl-C ( $p < 0.001$ ). It has been noted previously that, despite altering the polymer conformation, iota carrageenan is rheologically insensitive to cations.<sup>[48]</sup> This provides further evidence that that sprayability is not necessarily related to rheological properties in structured fluids.<sup>[44]</sup> However, with an 18-fold increase in spray area ( $p < 0.01$ ), the CaCl<sub>2</sub>-C formulation had the same spray coverage as the dilute solutions. This shows that creating discrete microparticles, rather than the continuous entangled network seen in concentrated polymer solutions, is paramount for sprayability (Figure 9C).

A final consideration is prevention of the initial stimulus that initiates the fibrotic cascade. In dystrophic EB, for example, minimal shear trauma can lead to progressive blistering, ulceration, and subsequent scarring, including on the internal mucosa. If shear trauma can be minimized by lubricating the oral mucosa, this may allow normal eating and oral hygiene, without leading to progressive scarring. The lubricating action of the formulations was thus investigated. The dilute system was a poor lubricant, displaying a reduction in friction only at high speeds, while both concentrated systems reduced the coefficient of friction at much lower speeds (Figure 9D). Interestingly, the microstructured system was significantly more lubricating than the iota carrageenan alone in solution at low speeds (Figure 9E,  $p < 0.01$ ). At high speeds, the lubrication ability of both concentrated systems was similar, though both significantly reduced friction compared to the dilute system ( $p < 0.05$ ).

### 3. Conclusions

All anionic polysaccharides tested, but not neutrally charged MC, were able to prevent or inhibit collagen fibrillogenesis, depending on concentration. In an in vitro model of fibrosis, many of the anionic polysaccharides had some effect, but iota carrageenan alone significantly downregulated COL1,  $\alpha$ SMA, SMAD3, and SMAD4 gene transcription, as well as COL1 and  $\alpha$ SMA protein



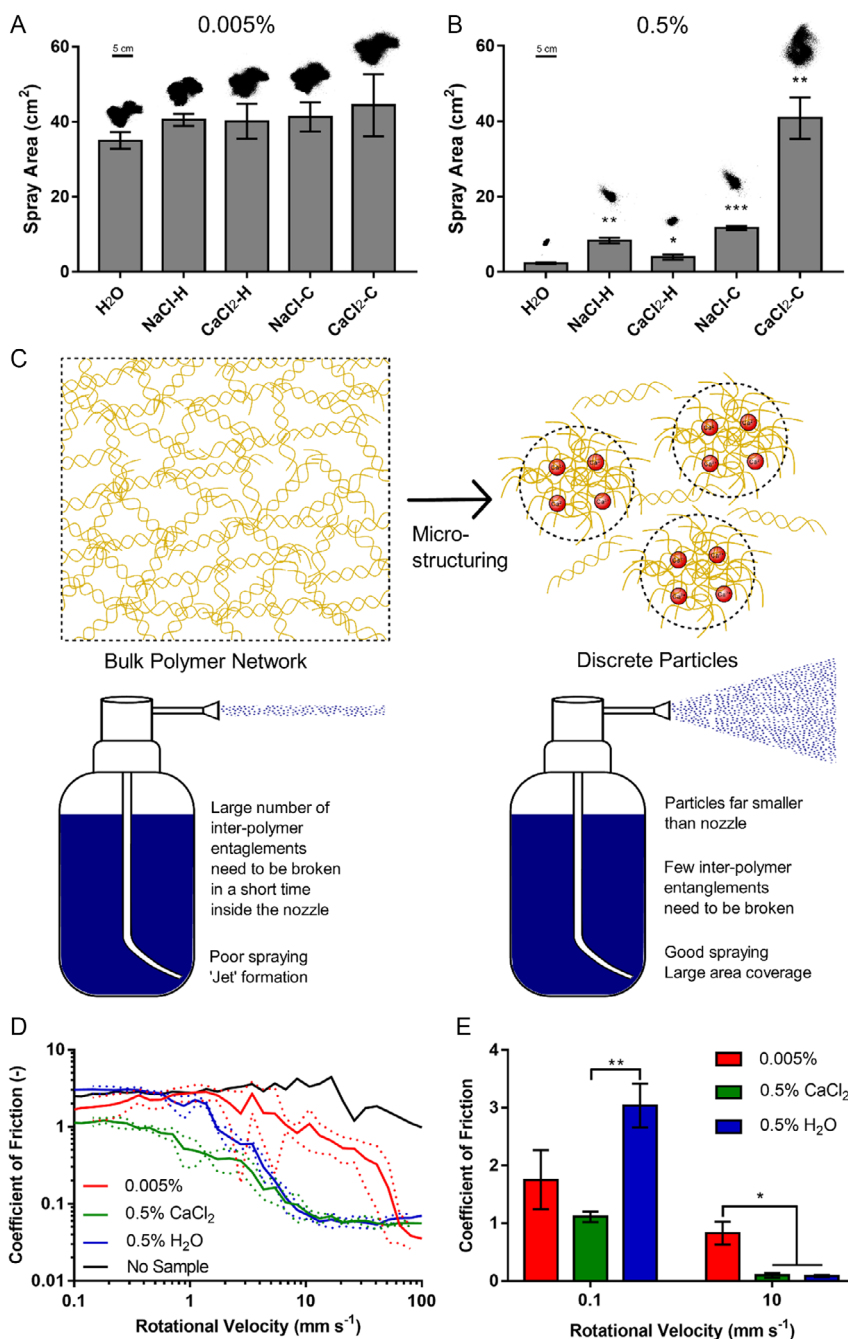


**Figure 9.** Spray and lubrication of iota carrageenan formulations. Spray coverage of formulations of A) 0.005% and B) 0.5% iota carrageenan, with a representative image of each distribution. C) Schematic showing the mechanism by which microstructuring a continuous entangled network into discrete particles leads to large increases in spray area. D) Friction curves for various formulations. E) Comparison of the coefficient of friction at 0.1 and 10 mm s<sup>-1</sup>. In (A) and (B), mean ± SD ( $n = 3$ ), statistical differences calculated using a  $t$ -test with Welch's correction between each group and H<sub>2</sub>O; in D), mean (solid line) ± SD (dotted lines) ( $n = 3$ ); in E) mean ± SD statistical differences calculated using a  $t$ -test with Welch's correction.

expression. This is likely due to iota carrageenan forming a complex with TGFβ1, preventing it from binding to cell receptors to initiate myofibroblast transdifferentiation. Iota carrageenan can be microstructured by adding calcium, but only when cold following double-helix formation. This microstructured formulation can be sprayed for high surface coverage, and provides a

lubricating effect. By preventing myofibroblast transdifferentiation at the molecular/cell level, inhibiting collagen laydown at the ECM level, and lubricating to limit shear-induced trauma at the macro level, iota carrageenan could present a promising new therapy to prevent the persistent oral scarring seen in EB.

## 4. Experimental Section

**Materials:** All water used was MilliQ type 1 deionized water unless otherwise stated. Collagen (type 1, rat tail) was purchased from Corning. Gellan (low acyl) was purchased from Kelcogel. Iota carrageenan (commercial grade), DS (sodium salt from *Leuconostoc spp.*, for molecular biology), Alg (BioReagent grade), MC, bovine serum albumin (BSA), sirius red, picric acid solution, acetic acid, sodium hydroxide, sodium chloride, and calcium chloride dihydrate were purchased from Sigma. TGFβ1 (human recombinant) was purchased from ProteinTech. Phosphate buffered saline (PBS), Dulbecco's Modified Eagle's Medium (DMEM), fetal bovine serum (FBS), penicillin, and streptomycin were purchased from Gibco.

**Collagen Fibrillogenesis:** All reagents were refrigerated at 4 °C before and throughout this protocol, to prevent fibrillogenesis occurring prior to incubation. Collagen was diluted from its initial concentration (3.71 mg mL<sup>-1</sup>) to 0.8 mg mL<sup>-1</sup> with deionized water. Polymer solutions were made by dissolving in deionized water at 0.5 w/v%, and concentrations of 0.005, 0.0005, and 0.00005 w/v% were made by serial dilution. 150 μL of 1 × PBS was placed to each well of a 96 well plate, and 75 μL of polymer solution was added, and mixed thoroughly by pipette mixing. Then, 75 μL of 0.8 mg mL<sup>-1</sup> collagen solution was added to each well, and was mixed thoroughly by pipette mixing, taking care to avoid the formation of bubbles. The plate was then placed in a plate reader (Spark, Tecan), which was preheated to 30 °C, and the 405 nm absorbance was read over 6 h. The data was normalized by dividing through by the initial absorbance value, and then analyzed by fitting an exponential plateau plus dead-time equation

$$A(t) = A_{\max} - (A_{\max} - A_0)e^{-k(t-t_d)} \quad (1)$$

where  $A(t)$  (–) is the normalized 405 nm absorbance as a function of time,  $A_{\max}$  (–) is the plateau value at infinite time,  $A_0$  (–) is the initial value (set to 1 as data is normalized),  $k$  (min<sup>-1</sup>) is a rate constant,  $t$  is the experiment time (min), and  $t_d$  is the dead time (min). This model was then used to find the time at which the absorbance reached 95% of the plateau value, by rearranging Equation (1)

$$t_{95\%} = t_d - \frac{1}{k} \ln \left( \frac{0.05A_{\max}}{A_{\max} - A_0} \right) \quad (2)$$

**Cell Culture:** Human dermal fibroblasts were purchased from Sigma. Adherent 2D cultures were maintained in high-glucose DMEM supplemented with 10% FBS, 2 mM L-glutamine, 100 U mL<sup>-1</sup> penicillin, and 0.1 mg mL<sup>-1</sup> streptomycin under 5% CO<sub>2</sub> at 37 °C. For experiments, this medium with 1% FBS was used to minimize the effects of unknown cytokines in the serum. When used, TGFβ1 was added directly to the media. To introduce polysaccharides, autoclaved solutions were made up a concentration on 0.1 wv<sup>-1</sup>% to supplement the DMEM at a 1 in 20 dilution, to achieve a final concentration of 0.005%.

**Gene Expression:** To ensure sufficient RNA harvest, cells were seeded in 6-well plates at a density of 150 000 cells per well, and allowed to settle for 72 h in DMEM with 10% FBS. Media was then changed to 1% FBS for 24 h to allow the cells to acclimatize. Experimental media, which was prepared 24 h in advance, was then applied for 48 h: NC was a replacement of 1% FBS DMEM; PC was 1% FBS DMEM plus 10 ng mL<sup>-1</sup> TGFβ1; the other experimental medias were 1% FBS DMEM plus 10 ng mL<sup>-1</sup> TGFβ1 and 0.005% gellan (G), iota carrageenan (iC), DS, Alg, or MC.

Cells were then lysed and RNA extracted using an RNEasy mini kit (Qiagen), and the purity checked by ensuring the 260/280 absorbance ratio was ≥2, before converting to cDNA using a high-capacity cDNA reverse transcription kit (Applied Biosystems), following the manufacturer's instructions. Gene expression analysis was performed on each sample for COL1, αSMA, SMAD3, SMAD4, and glyceraldehyde-3-phosphate dehydrogenase (GAPDH) (housekeeper), using an SYBR green (Applied Biosystems)-based RT-qPCR, with QuantiTect primer assays (Qiagen) and an AriaMx Real-Time PCR system (Agilent Technologies). qRT-PCR data were analyzed using the Delta-Delta Ct method as

described previously<sup>[52]</sup> with the NC samples used as the calibrator and GAPDH as the endogenous control gene. Relative quantification values are presented as fold changes in gene expression relative to the control group, which was normalized to one.

**Protein Expression:** Cells were seeded in 8-well chamber slides at a density of 5000 cells per well, and allowed to settle for 72 h in DMEM with 10% FBS. Media was replaced with 1% FBS for 24 h to allow the cells to acclimatize. For 2-day experiments (data presented in Figure 5A–C), the experimental media was prepared 24 h in advance, and then applied for 48 h; experimental media are described earlier. For 2-day experiments assessing the inhibition mechanism (data presented in Figure 4A), the same procedure was followed, but the experimental media was prepared immediately prior to application. For 5-day experiments (data presented in Figure 3D), group NC1 was treated with 1% FBS DMEM, and all other experimental groups were treated with 1% FBS DMEM plus 10 ng mL<sup>-1</sup> TGFβ1, for 48 h. The media was then changed again: groups NC1 and NC2 had 1% FBS DMEM, group PC had 1% FBS DMEM plus 10 ng mL<sup>-1</sup> TGFβ1, and the remaining groups had 1% FBS DMEM plus 0.005% of their respective polymer. These conditions were retained for 72 h, with a change of media at 48 h.

For immunocytochemical analysis, cells were washed with PBS, fixed with 10% formalin at ambient temperature for 10 min, and then washed again with PBS. Cells were blocked with 0.1% triton X-100, 3% BSA in PBS, for 30 min. Antibodies were made up in 0.5% Tween 20, 3% BSA in PBS. Primary antibodies for collagen 1 (polyclonal rabbit, Abcam) and αSMA (monoclonal mouse, Sigma) were made up 1 in 200, and added to each well for 1 h. Secondary antibodies (594 goat anti-rabbit and 488 goat anti-mouse, Alexa Fluor, Invitrogen) were made up 1 in 500 and, following PBS washing, added up each well for 1 h, protecting from light. Finally, each well was washed with PBS, DAPI was added for 10 min to stain nuclei, and wells were washed again before the chamber was removed and a cover slip applied to the slides. Cells were imaged using an Evos M5000 fluorescent microscope equipped with a dark box, ensuring the same camera settings for every image. Fluorescence intensity quantification was carried out in ImageJ, thresholding to remove all areas not containing cells, then assessing the average intensity of the remaining area.

For picosirius red staining, cells were washed with PBS, then fixed in methanol overnight at –20 °C. Wells were washed with PBS again, then stained with picosirius red (0.1% sirius red in saturated picric acid) at ambient temperature for 1 h. Wells were then washed with 0.1% acetic acid five times to remove nonspecifically bound stain. The collagen-bound stain was then eluted with 0.1 M NaOH, and the absorbance of the eluent was read at 540 nm in a plate reader (Spark, Tecan).

**Dynamic Light Scattering:** To replicate the conditions in the cell experiments as far as possible, DMEM (without phenol red indicator as this may interfere with measurement) was used as the dispersant medium. TGFβ1 was dispersed at a concentration of 0.0005 g L<sup>-1</sup> (500 ng mL<sup>-1</sup>) to achieve a measurable concentration. iC was prepared as in the cell experiments mentioned earlier, and added to the DMEM with and without TGFβ1. Samples were made 24 h before measurement, to replicate conditions in the cell experiments. Particle size was measured by dynamic light scattering (DLS), using a Zetasizer (Nano ZS, Malvern).

**Iota Carrageenan Formulation:** Stock iota carrageenan solution was made by dissolving at a concentration 0.555 w/v% in deionized water at 80 °C, which was diluted 100-fold for the stock dilute solution. Sodium chloride and calcium chloride solutions were made at a concentration of 5 M in volumetric flasks. To prepare formulations, 45 mL of stock solution was stirred at 1200 rpm, and 5 mL of water or salt solution was added (resulting in final concentrations of 0.5% or 0.005% iota carrageenan, and 0.5 M salt, where added). For “hot mixes,” denoted “H,” the salt was added while the iota carrageenan solution was still at 80 °C, and was then stirred for 30 min until cool. For “cold mixes,” denoted “C,” the iota carrageenan was allowed to cool down to room temperature, and then the salt solution was added under stirring.

**Light Microscopy:** A drop of each formulation was placed on a microscope slide, covered with a glass cover slip, and imaged using a light microscope (Evos XL Core).

**Turbidity:** 1 mL of formulation was syringed into a 48-well plate, and the absorbance at 350 nm was measured using a plate reader (Spark, Tecan).

**Rheology:** Rheological characterization was carried out on a Kinexus Ultra+ (Netzsch), at 25 °C. For dilute samples (0.005%), a double-gap geometry was used to maximize contact area, and for concentrated samples (0.5%), a parallel plate geometry with a 1 mm gap. Oscillatory tests were carried out at a strain of 0.5%, derived from an amplitude sweep. Stress ramps were carried out from 0.01 to 100 Pa, over 10 min.

**Sprayability:** Formulations were mixed with 0.001% rhodamine 6 G for visualization, and then loaded into a standard hand-pump spray bottle. The pump was primed, and then sprayed vertically downward onto A5 paper from a distance of 5 cm. Once dried, the paper was imaged using a fluorescent scanner (iBright 1500, Invitrogen), and images were loaded in ImageJ, cropped, thresholded, and particle analysis carried out to assess the percentage area of the cropped square, which was then converted to a real surface area.

**Tribology:** Lubrication was assessed using a three-ball tribological attachment for the rheometer, with silicone elastomer (Sylgard 184, Dow) used as the lower surface. Formulation was added so as to cover the lower surface. A normal force of 1 N was employed, and tests were carried out at 25 °C. The upper geometry was accelerated from 0.1 to 10 mm s<sup>-1</sup>.

## Acknowledgements

This work was funded by DEBRA UK and Ireland.

## Conflict of Interest

The authors declare no conflict of interest.

## Data Availability Statement

The data that support the findings of this study are available from the corresponding author upon reasonable request.

## Keywords

alpha smooth muscle actin, collagen fibrillogenesis, lubrication, myofibroblast transdifferentiation, polysaccharide, scarring, transforming growth factor beta 1 pathway

Received: May 5, 2023

Revised: June 28, 2023

Published online:

- [1] S. M. Karppinen, R. Heljasvaara, D. Gullberg, K. Tasanen, T. Pihlajaniemi, *F1000Res* **2019**, *8*, 787.
- [2] A. D. Metcalfe, M. W. J. Ferguson, *J. R. Soc. Interface* **2006**, *4*, 413.
- [3] J. Q. Coentro, E. Pugliese, G. Hanley, M. Raghunath, D. I. Zeugolis, *Adv. Drug Deliv. Rev.* **2019**, *146*, 37.
- [4] O. Bock, G. Schmid-Ott, P. Malewski, U. Mrowietz, *Arch. Dermatol. Res.* **2006**, *297*, 433.
- [5] B. C. Brown, S. P. McKenna, K. Siddhi, D. A. McGrouther, A. Bayat, *J. Plast. Reconstr. Aesthet. Surg.* **2008**, *61*, 1049.
- [6] N. E. E. Van Loey, M. J. M. Van Son, *Am. J. Clin. Dermatol.* **2003**, *4*, 245.
- [7] N. L. Ocleston, A. D. Metcalfe, A. Boanas, N. J. Burgoyne, K. Nield, S. O'Kane, M. W. J. Ferguson, *Dermatol. Res. Pract.* **2010**, *2010*, 1.
- [8] S. Saika, O. Yamanaka, T. Sumioka, T. Miyamoto, K. i. Miyazaki, Y. Okada, A. Kitano, K. Shirai, S. i. Tanaka, K. Ikeda, *Prog. Retinal Eye Res.* **2008**, *27*, 177.
- [9] J. P. Whitcher, M. Srinivasan, M. P. Upadhyay, *Bull. World Health Organ.* **2001**, *79*, 214.
- [10] D. Chanda, E. Otoupalova, S. R. Smith, T. Volckaert, S. P. De Langhe, V. J. Thannickal, *Mol. Aspects Med.* **2019**, *65*, 56.
- [11] T. Kisseleva, D. Brenner, *Nat. Rev. Gastroenterol. Hepatol.* **2020**, *18*, 151.
- [12] S. Djurdjaj, P. Boor, *Mol. Aspects Med.* **2019**, *65*, 16.
- [13] N. C. Henderson, F. Rieder, T. A. Wynn, *Nature* **2020**, *587*, 555.
- [14] B. Carey, J. Setterfield, *Clin. Exp. Dermatol.* **2019**, *44*, 732.
- [15] C. Scully, L. Lo Muzio, *Br. J. Oral Maxillofac. Surg.* **2008**, *46*, 358.
- [16] A. Bardhan, L. Bruckner-Tuderman, I. L. C. Chapple, J. D. Fine, N. Harper, C. Has, T. M. Magin, M. P. Marinkovich, J. F. Marshall, J. A. McGrath, J. E. Mellerio, R. Polson, A. H. Heagerty, *Nat. Rev. Dis. Primers* **2020**, *6*, 78.
- [17] E. Luo, H. Liu, Q. Zhao, B. Shi, Q. Chen, *Int. J. Oral Sci.* **2019**, *11*, 9.
- [18] Y. Liu, Y. Li, N. Li, W. Teng, M. Wang, Y. Zhang, Z. Xiao, *Sci. Rep.* **2016**, *6*, 32231.
- [19] J. L. Xie, S. H. Qi, S. Pan, Y. Bin Xu, T. Z. Li, X. S. Liu, P. Liu, *Dermatol. Surg.* **2008**, *34*, 1216.
- [20] A. C. Midgley, M. Rogers, M. B. Hallett, A. Clayton, T. Bowen, A. O. Phillips, R. Steadman, *J. Biol. Chem.* **2013**, *288*, 14824.
- [21] K. L. Walton, K. E. Johnson, C. A. Harrison, *Front. Pharmacol.* **2017**, *8*, 461.
- [22] T. Krieg, M. Heckmann, *Recenti Prog Med* **1989**, *80*, 594.
- [23] R. J. Diebold, M. J. Eis, M. Yin, I. Ormsby, G. P. Boivini, B. J. Darrow, J. E. Saffitz, T. Doetschman, *Proc. Natl. Acad. Sci. U S A* **1995**, *92*, 12215.
- [24] R. J. Akhurst, A. Hata, *Nat. Rev. Drug Discov.* **2012**, *11*, 790.
- [25] D. Qureshi, A. K. Nayak, D. Kim, S. Maji, A. Anis, B. Mohanty, K. Pal, in *Advances and Challenges in Pharmaceutical Technology: Materials, Process Development and Drug Delivery Strategies*, Academic Press, Cambridge, MA **2021**, pp. 283–325.
- [26] T. G. Barclay, C. M. Day, N. Petrovsky, S. Garg, *Carbohydr. Polym.* **2019**, *221*, 94.
- [27] A. Sarraf, E. Verton, N. Addoun, Z. Boual, M. D. Ould El Hadj, Z. El Alaoui-Talibi, C. El Modafar, S. Abdelkafi, I. Fendri, C. Delattre, P. Dubessay, P. Michaud, G. Pierre, *Appl. Sci.* **2021**, *11*, 5243.
- [28] S. Ullah, A. A. Khalil, F. Shaukat, Y. Song, *Foods* **2019**, *8*, 304.
- [29] P. Maity, I. K. Sen, I. Chakraborty, S. Mondal, H. Bar, S. K. Bhanja, S. Mandal, G. N. Maity, *Int. J. Biol. Macromol.* **2021**, *172*, 408.
- [30] J. R. Barbosa, R. N. de Carvalho Junior, *Trends Food Sci. Technol.* **2021**, *108*, 223.
- [31] Y. Yu, M. Shen, Q. Song, J. Xie, *Carbohydr. Polym.* **2018**, *183*, 91.
- [32] X. Yang, A. Li, X. Li, L. Sun, Y. Guo, *Trends Food Sci. Technol.* **2020**, *102*, 1.
- [33] M. Ghebremedhin, S. Seiffert, T. A. Vilgis, *Curr. Res. Food Sci.* **2021**, *4*, 436.
- [34] B. ter Horst, R. J. A. Moakes, G. Chouhan, R. L. Williams, N. S. Moiemem, L. M. Grover, *Acta Biomater.* **2019**, *89*, 166.
- [35] I. Fernández Farrés, M. Douaire, I. T. Norton, *Food Hydrocolloids* **2013**, *32*, 115.
- [36] X. Cheng, P. M. Pinsky, *J. R. Soc. Interface* **2013**, *10*, 20130512.
- [37] D. Chen, L. R. Smith, G. Khandekar, P. Patel, C. K. Yu, K. Zhang, C. S. Chen, L. Han, R. G. Wells, *Sci. Rep.* **2020**, *10*, 19065.
- [38] C. C. Reed, R. V. Iozzo, *Glycoconjugate J.* **2002**, *19*, 249.
- [39] C. H. Heldin, K. Miyazono, P. Ten Dijke, *Nature* **1997**, *390*, 465.
- [40] K. Yanagisawa, H. Osada, A. Masuda, M. Kondo, T. Saito, Y. Yatabe, K. Takagi, T. Takahashi, T. Takahashi, *Oncogene* **1998**, *17*, 1743.

- [41] G. S. Ashcroft, X. Yang, A. B. Glick, M. Weinstein, J. J. Letterio, D. E. Mizel, M. Anzano, T. Greenwell-Wild, S. M. Wahl, C. Deng, A. B. Roberts, *Nat. Cell Biol.* **1999**, *1*, 260.
- [42] G. Dabiri, D. A. Tumbarello, C. E. Turner, L. Van De Water, *J. Invest. Dermatol.* **2008**, *128*, 280.
- [43] A. P. Popova, P. D. Bozyk, A. M. Goldsmith, M. J. Linn, J. Lei, J. K. Bentley, M. B. Hershenson, *Am. J. Physiol. Lung Cell Mol. Physiol.* **2010**, *298*, L735.
- [44] T. E. Robinson, R. A. J. Moakes, L. M. Grover, *Front Med. Technol.* **2021**, *3*, 25.
- [45] A. S. Michel, M. M. Mestdagh, M. A. V. Axelos, *Int. J. Biol. Macromol.* **1997**, *21*, 195.
- [46] V. Evageliou, A. Gerolemou, A. Zikas, A. Basios, M. Komaitis, *Int. J. Food Sci. Technol.* **2011**, *46*, 1001.
- [47] V. T. N. T. Bui, B. T. Nguyen, T. Nicolai, F. Renou, *Carbohydr. Polym.* **2019**, *223*, 115107.
- [48] T. Funami, M. Hiroe, S. Noda, I. Asai, S. Ikeda, K. Nishinari, *Food Hydrocolloids* **2007**, *21*, 617.
- [49] M. Tako, S. Nakamura, Y. Kohda, *Carbohydr. Res.* **1987**, *161*, 247.
- [50] Y. Yuguchi, H. Urakawa, K. Kajiwara, *Food Hydrocolloids* **2003**, *17*, 481.
- [51] S. Janaswamy, R. Chandrasekaran, *Carbohydr. Res.* **2002**, *337*, 523.
- [52] K. J. Livak, T. D. Schmittgen, *Methods* **2001**, *25*, 402.